Heterogeneous Seed-Assisted $FAPbI_3$ Crystallization for Efficient Inverted Perovskite Solar Cells

*Nan Yan,[1] Yang Cao,[1] Zhonghua Dai,[1] Long Jiang,[3] Yuanbo Yang,[3] Tiantian Li,[3] Liwei Li,[3] Shengzhong (Frank) Liu,[1,4]*Zhimin Fang,[2,]* Jiangshan Feng[1,]**

N. Yan, Y. Cao, Z. Dai, Prof. S. Liu, J. Feng

Key Laboratory of Applied Surface and Colloid Chemistry, Ministry of Education, Shaanxi Key Laboratory for Advanced Energy Devices, Shaanxi Engineering Lab for Advanced Energy Technology, School of Materials Science and Engineering, Shaanxi Normal University, Xi'an 710119, China

E-mail: fengjs@snnu.edu.cn;

E-mail: szliu@dicp.ac.cn

Z. Fang

Institute of Technology for Carbon Neutralization, Yangzhou University, Yangzhou, 225127, China

E-mail: fangzm@yzu.edu.cn

L. Jiang, Y. B. Yuan, T. T. Li, L. W. Li

State Key Laboratory of Oil and Gas Equipment, CNPC Tubular Goods Research Institute, Xi'an, Shaanxi 710077, China

Prof. S. Liu

University of Chinese Academy of Sciences, Dalian Institute of Chemical Physics, Chinese Academy of Sciences, Dalian, 116023, China

Keywords: inverted perovskite solar cell, δ-$FAPbI_3$, α-$FAPbI_3$, nucleation, crystal growth

Methods

Materials

Cesium Iodide (CsI, >99.9%), phenyl-C_{61}-butyricacidmethylester ($PC_{61}BM$, 98%), N4'-bis(4-ethenylphenyl)-N4, N4'-di-1-naphthalenyl-[1,1'-biphenyl]-4,4'-diamine (VNPB) and bathocuproine (BCP, >99%) were purchased from Xi'an uri Solar Co. Ltd. Methylammonium iodide (MABr) and methylamine chloride (MACl), formamidinium iodid (FAI) were purchased from Xi'an Nengcai Photoelectronic Technology Co., Ltd. Lead(II) iodide (PbI_2, 99.999%). N, N-dimethylformamide (DMF) (>99.9%), dimethyl sulfoxide (DMSO) (>99.9%), anhydrous ethyl acetate (EA), isopropanol (IPA) and Chlorobenzene (CB) were purchased from Advanced Election Technilogy Co., Ltd.

Solar cell device Fabrication

The FTO substrates were cleaned by ultrasonics in detergent, deionized water, ethanol sequentially. After that, the FTO substrates were transferred into an electron beam evaporation system to evaporated 25 nm NiO_x films. O_2 plasma treatments were carried out the prepered NiO_x films in a vacuum plasma cleaning system. The prepared substrates were then transferred to a glove box and coated with a thin layer of VNPB (1 mg/mL in chlorobenzene) at 6000 rpm for 30 s, followed by annealing at 120 °C for 10 min. For the synthesis of the perovskite precursor, a mixture of 1.5 M $Cs_{0.02}(FA_{0.98}MA_{0.02})_{0.98}Pb(I_{0.99}Br_{0.01})_3$ perovskite, DMF/DMSO solvent (with a volumetric ratio of 5:1), 5% excess PbI_2, and 30% MACl was vigorously stirred overnight at room temperature. The resulting precursor solutions were filtered through a 0.20-μm PTFE membrane before use, and subsequently spin-coated onto the VNPB layer at 1000 rpm for 10 s and 4000 rpm for 40 s. During the second step of the spin-coating process, 150 μL of EA was dropped onto the spinning substrate

at 15 s prior to completion. The substrates were then annealed at 110 °C for 20 min. A $PC_{61}BM$ layer was subsequently deposited onto the perovskite film by spin-coating a 20 mg/mL chlorobenzene solution at 4000 rpm for 30 s. A BCP solution (0.5 mg/mL in IPA) was then spin-coated onto the $PC_{61}BM$ layer at 4000 rpm for 30 s. Finally, an Ag layer (~80 nm) was evaporated onto the prepared films using a shadow mask under high vacuum conditions (approximately 10^{-5} Pa). To minimize reflection, a 100 nm MgF_2 layer was evaporated onto the glass side of the FTO substrates. The active area of the solar cells employed in this study was 0.09 cm^2.

Film Characterization

X-ray diffraction (XRD) patterns were acquired using a D/MAX 2400 diffractometer equipped with Cu Kα radiation (1.5405 Å). For the XRD analysis, glass substrates were spin-coated with FAI or PbI_2 solutions (DMF/DMSO) in the presence and absence of DAP molecules. To assess the morphology of the perovskite film, scanning electron microscopy (SEM) was performed using a HITACHI SU-8020 instrument. The surface roughness of the perovskite films was evaluated through atomic force microscopy (AFM) using a Bruker Dimension Icon (Bruker Nano, Inc.) instrument. The water contact angle measurements were conducted on a KRUSS DSA100 instrument under uniform LED illumination. X-ray photoelectron spectroscopy (XPS) and ultraviolet photoelectron spectroscopy (UPS) measurements were carried out using an ESCALAB $250Xi^+$ instrument to examine the surface elements and energy levels of the perovskite material. The steady-state photoluminescence (PL) and UV-vis absorption spectra were recorded using an FLS980 spectrometer (Edinburgh Instruments Co., Ltd.) and a UV-visible spectrophotometer (HITACHI-UH4150), respectively. Time-of-flight secondary ion mass spectrometry (TOF-SIMS) analysis was performed

with an IONTOF GmbH (Germany) instrument (Model: M6). Liquid-state ^{1}H NMR analysis was conducted on a 400 MHz nuclear magnetic resonance spectrometer (JNM-ECZ400R/S1, Japan) using d6-DMSO as the deuterated solvent. Fourier transform infrared spectra were obtained using a Brooke-VERSEX 70 instrument (Germany).

Device Characterizations

The current density-voltage (*J-V*) measurements were obtained at ambient conditions using a Keithley 2400 source. The simulated AM 1.5G illumination (100 $mWcm^{-2}$) was provided by a xenon-lamp-based solar simulator, with the device active area measuring 0.09 cm^2. The EQE measurements were carried out using the QTest Station 2000 ADI system (Crowntech, Inc.). Dark state J-V measurements were performed using the Keithley 2400 source under dark conditions. The trap densities and carrier mobilities were estimated employing the space-charge-limited current (SCLC) approach via the Keithley 2400 source. Electrochemical impedance spectroscopy (EIS) and capacitance-voltage (C-V) measurements were conducted in the dark using a ModuLab XM CHAS 08 instrument. The frequency range of these measurements spanned from 0.1 Hz to 100 MHz.

Theoretical calculation

The optimization of the structure and electrostatic potentials for DAP•PbI_2 and DAP•FAI were performed using DFT calculations implemented in the Gaussian software package. In order to accurately account for the intermolecular interaction within the complexes, the DFT calculations were conducted with the ωB9X-D functional and the Def2TZV basis set.

The DFT calculations were conducted utilizing the Vienna Ab initio Simulation Package (VASP),

incorporating the projected augmented wave (PAW) method [1] and employing a plane-wave basis set [2]. The electronic exchange-correlation interaction was described using the Perdew-Burke-Ernzerhof (PBE) functional [3] under the generalized gradient approximation (GGA). All calculations employed an energy cutoff of 420 eV and only relied on a gamma *k*-point grid centered at gamma. To calculate the binding energy of DAP molecules on the surfaces of δ-$FAPbI_3$, 2×2×3 supercells of δ-$FAPbI_3$ perovskites were constructed. Then, the DAP molecule was inserted into the (001) surfaces of the perovskites. To prevent periodic interactions in the *z*-direction, a vacuum layer of 35 Å thickness is implemented. The van der Waals interactions between the $FAPbI_3$ and DAP were taken into account using the D3 correction [4] with the Becke-Jonson damping function. With a fixed portion of substrate atoms, the structures were optimized by relaxing the top adsorbed cluster molecules. All the computations employed the 10^{-5} eV and 0.1 eV $Å^{-1}$ as the energy and force convergence criteria, respectively. The surface binding energy for adsorbent A on substrate B is calculated as $E_b=E_{A/B}-E_A-E_B$ where $E_{A/B}$, E_A and E_B are the energies of the adsorbing system A/B (see Fig. S4 for δ-$FAPbI_3$ systems), isolated adsorbent A (δ-$FAPbI_3$) and B (DAP), respectively[5].

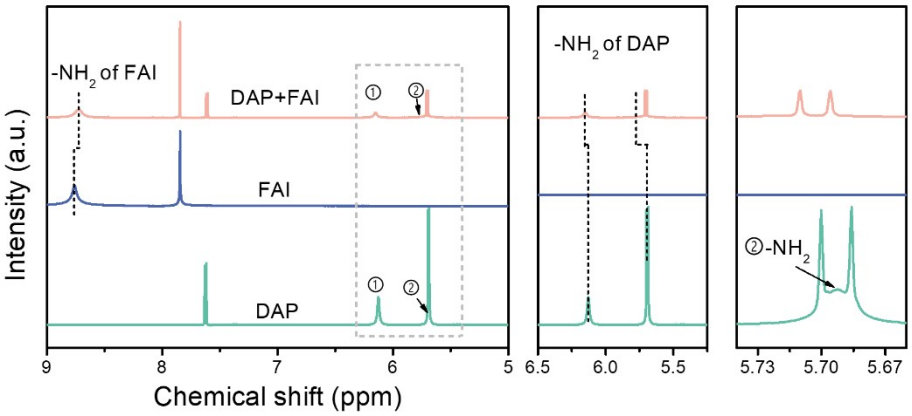

Fig. S1. ^{1}H NMR spectra of DAP, FAI, and DAP +FAI solution (d6-DMSO).

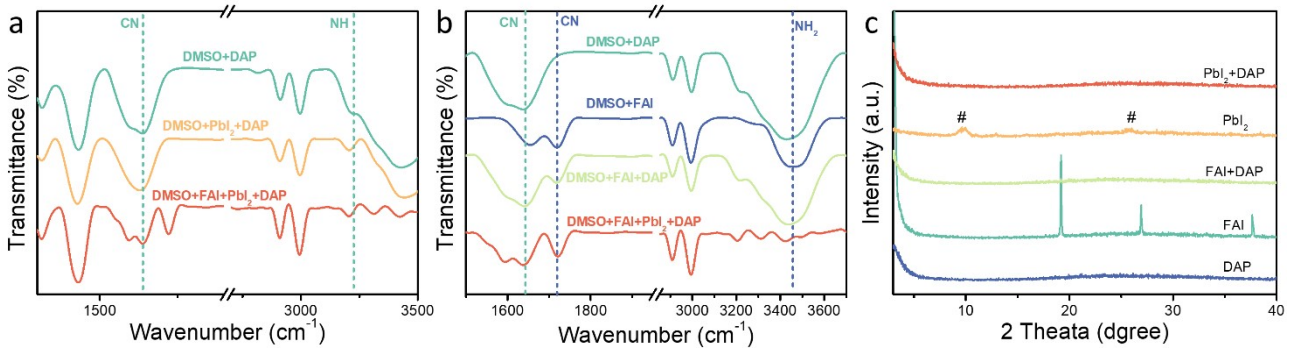

Fig. S2. (a, b) FTIR spectra of DAP, DAP+PbI_2, FAI, DAP+FAI and DAP+PbI_2+FAI solution (DMSO). (c) XRD patterns of FAI, PbI_2, FAI+DAP and PbI_2+DAP wet films without annealing. (the solvent of those wet film is the DMF/DMSO, # is the PbI_2·solvent complex.)

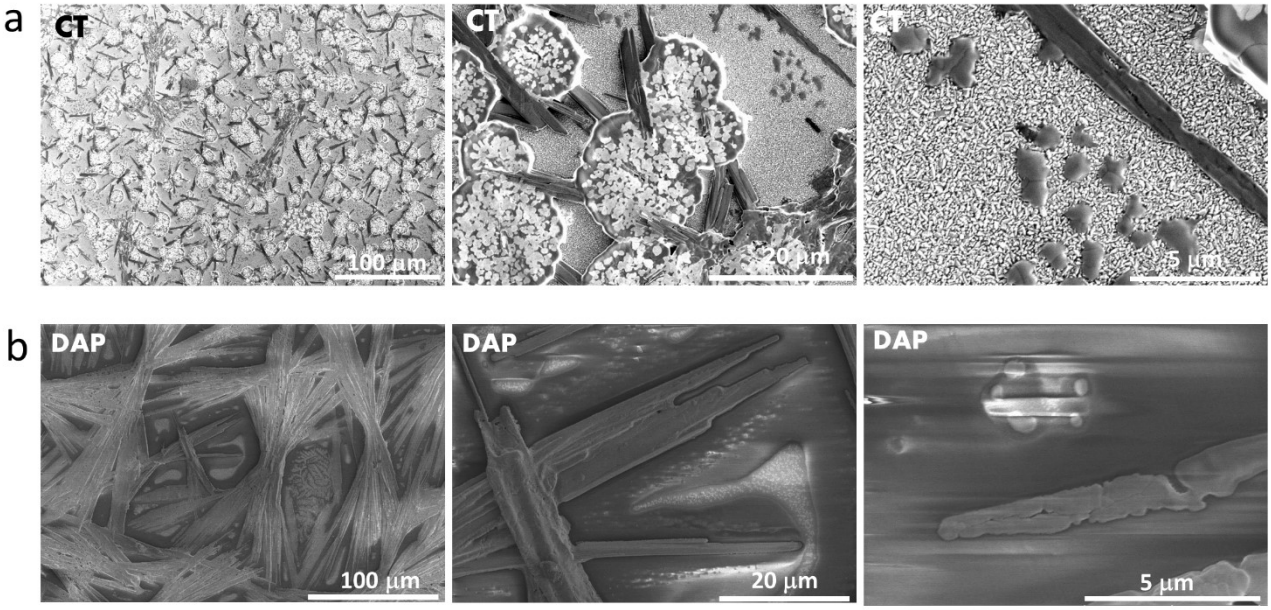

Fig. S3. SEM images of CT and DAP wet films without anti-solvent.

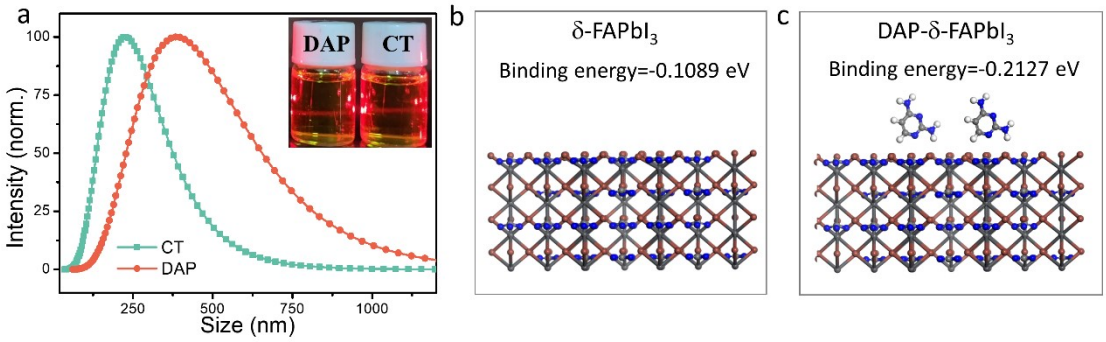

Fig. S4. (a) Dynamic light scattering (DLS) characterization and dingdall effect for the CT and DAP perovskite precursor solution. (b, c) The crystal models and corresponding binding energy of δ-$FAPbI_3$ and DAP-δ-$FAPbI_3$.

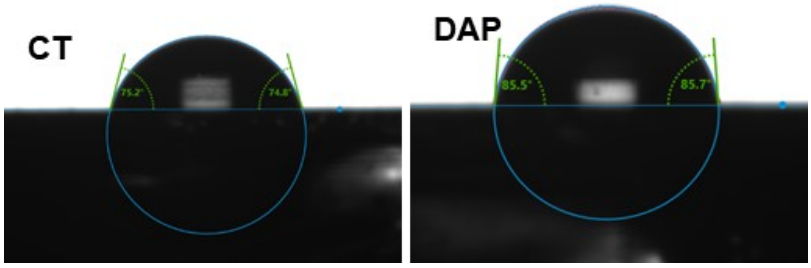

Fig. S5. Water contact angle of CT and DAP films.

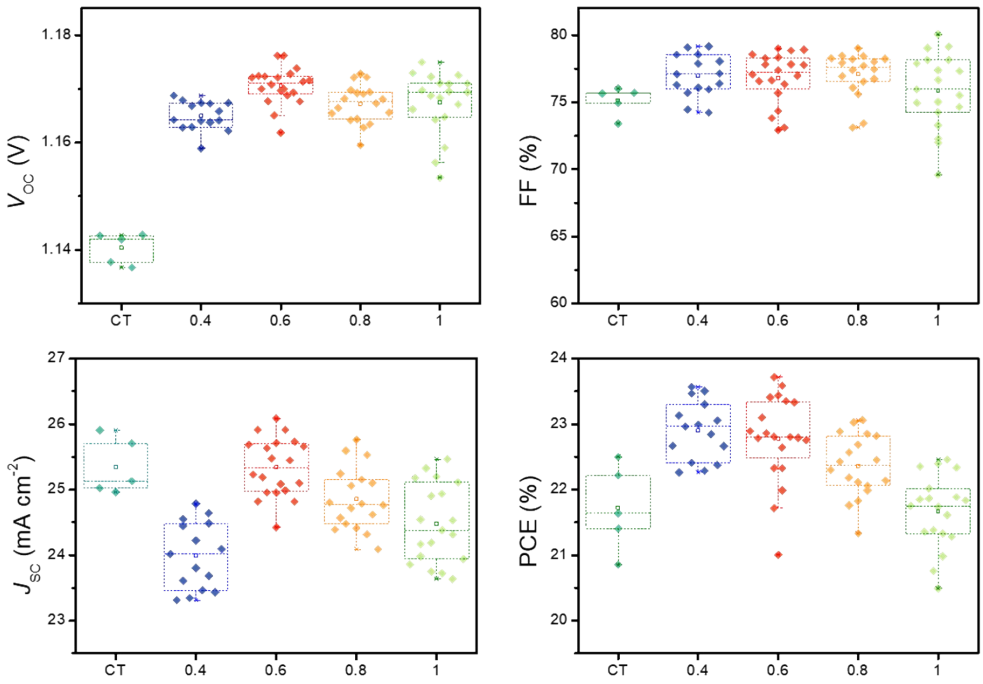

Fig. S6. PV parameters of devices with different concentration of DAP (0.4, 0.6, 0.8 and 1 mg/mL).

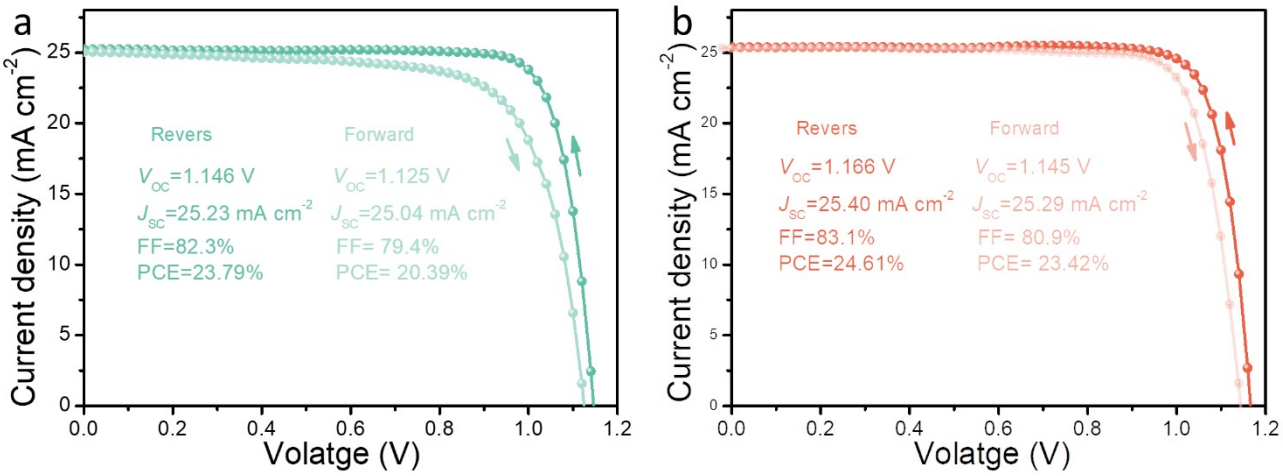

Fig.S7. The hysteresis of CT and DAP devices.

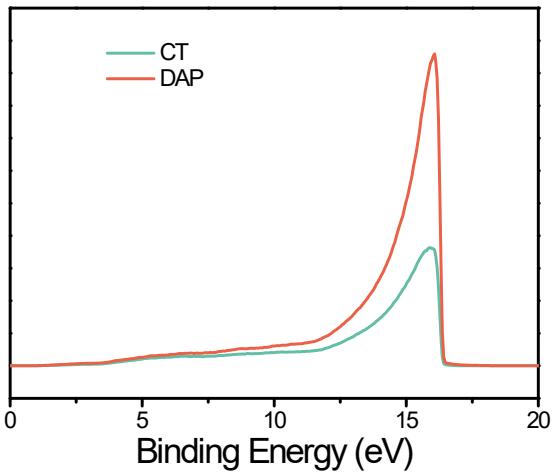

Fig. S8. UPS spectra obtained from CT and DAP perovskite films.

Table S1. The fitted parameters of PL lifetimes from the TRPL spectra.

Sample	τ_1(μs)	A1	τ_2(μs)	A2	τ_{ave}(μs)
CT	0.013	1416	1.29	6237	1.29
DAP	0.015	991	2.36	6323	2.36

Table S2. The fitted parameters of Nyquist plots from EIS characterization

Sample	Control	DAP
Rs (ohm)	31.89	23.04
Rct (ohm)	7141	6294

Reference

[1] P. E. Blöchl, *Physical Review B* 1994, **50**, 17953.

[2] G. Kresse, J. Furthmüller, *Computational Materials Science* 1996, **6**, 15.

[3] J. P. Perdew, K. Burke, M. Ernzerhof, *Phys Rev Lett* 1996, **77**, 3865.

[4] S. Grimme, J. Antony, S. Ehrlich, H. Krieg, *The Journal of chemical physics* 2010, **132**, 154104.

[5] Y. Guo, S. Apergi, N. Li, M. Chen, C. Yin, Z. Yuan, F. Gao, F. Xie, G. Brocks, S. Tao, N. Zhao, *Nature Communications* 2021, **12**, 644.